Rictor in perivascular adipose tissue controls vascular function by regulating inflammatory molecule expression

Bhattacharya, Indranil ; Drägert, Katja ; Albert, Verena ; Contassot, Emmanuel ; Damjanovic, Marlen ; Hagiwara, Asami ; Zimmerli, Lukas ; Humar, Rok ; Hall, Michael N ; Battegay, Edouard J ; Haas, Elvira

Abstract: OBJECTIVE: Perivascular adipose tissue (PVAT) wraps blood vessels and modulates vasoreactivity by secretion of vasoactive molecules. Mammalian target of rapamycin complex 2 (mTORC2) has been shown to control inflammation and is expressed in adipose tissue. In this study, we investigated whether adipose-specific deletion of rictor and thereby inactivation of mTORC2 in PVAT may modulate vascular function by increasing inflammation in PVAT. APPROACH AND RESULTS: Rictor, an essential mTORC2 component, was deleted specifically in mouse adipose tissue (rictor(ad-/-)). Phosphorylation of mTORC2 downstream target Akt at Serine 473 was reduced in PVAT from rictor(ad-/-) mice but unaffected in aortic tissue. Ex vivo functional analysis of thoracic aortae revealed increased contractions and impaired dilation in rings with PVAT from rictor(ad-/-) mice. Adipose rictor knockout increased gene expression and protein release of interleukin-6, macrophage inflammatory protein-1 , and tumor necrosis factor- in PVAT as shown by quantitative real-time polymerase chain reaction and Bioplex analysis for the cytokines in the conditioned media, respectively. Moreover, gene and protein expression of inducible nitric oxide synthase was upregulated without affecting macrophage infiltration in PVAT from rictor(ad-/-) mice. Inhibition of inducible nitric oxide synthase normalized vascular reactivity in aortic rings from rictor(ad-/-) mice with no effect in rictor(fl/fl) mice. Interestingly, in perivascular and epididymal adipose depots, high-fat diet feeding induced downregulation of rictor gene expression. CONCLUSIONS: Here, we identify mTORC2 as a critical regulator of PVAT-directed protection of normal vascular tone. Modulation of mTORC2 activity in adipose tissue may be a potential therapeutic approach for inflammation-related vascular damage.

DOI: https://doi.org/10.1161/ATVBAHA.112.301001

Rictor in Perivascular Adipose Tissue Controls Vascular Function by Regulating Inflammatory Molecule Expression

Indranil Bhattacharya[1], Katja Drägert[1], Verena Albert[2], Emmanuel Contassot[3], Marlen Damjanovic[1], Asami Hagiwara[2], Lukas Zimmerli[1], Rok Humar[1,4], Michael N. Hall[2], Edouard J. Battegay[1,4], Elvira Haas[1]

[1] Research Unit, Division of Internal Medicine, University Hospital Zurich, CH-8091 Zurich, Switzerland

[2] Biozentrum, University of Basel, CH-4046 Basel, Switzerland

[3] Division of Dermatology, University Hospital Zurich, CH-8091 Zürich, Switzerland

[4] Zurich Center for Integrative Human Physiology, CH-8057 Zürich, Switzerland

Word count of body: 4783

Word count of abstract: 227 (250 max)

Total number of figures: 6

Total number of tables: 0

Correspondence to:
Elvira Haas
Research Unit, Division of Internal Medicine
University Hospital Zurich
Gloriastr. 30
CH-8091 Zurich, Switzerland

Email: Elvira.haas@usz.ch
Phone: +41 446345335
FAX: +41 446345339

Abstract

Objective: Perivascular adipose tissue (PVAT) wraps blood vessels and modulates vasoreactivity by secretion of vasoactive molecules. Mammalian target of rapamycin complex 2 (mTORC2) has been shown to control inflammation and is expressed in adipose tissue. In this study, we investigated whether adipose-specific deletion of rictor and thereby inactivation of mTORC2 in PVAT, may modulate vascular function by increasing inflammation in PVAT.

Approach and Results: Rictor, an essential mTORC2 component, was deleted specifically in mouse adipose tissue (rictor$^{ad-/-}$). Phosphorylation of mTORC2 downstream target Akt at Serine 473 was reduced in PVAT from rictor$^{ad-/-}$ mice but unaffected in aortic tissue. Ex vivo functional analysis of thoracic aortae revealed increased contractions and impaired dilation in rings with PVAT from rictor$^{ad-/-}$ mice. Adipose rictor knockout increased gene expression and protein release of interleukin-6, macrophage inflammatory protein1α and tumor necrosis factorα in PVAT as shown by quantitative real-time PCR and Bioplex-analysis for the cytokines in the conditioned media, respectively. Moreover, gene and protein expression of iNOS was upregulated without affecting macrophage infiltration in PVAT from rictor$^{ad-/-}$ mice. Inhibition of iNOS normalized vascular reactivity in aortic rings from rictor$^{ad-/-}$ mice with no effect in rictor$^{fl/fl}$ mice. Interestingly, in perivascular and epididymal adipose depots, high-fat diet feeding induced downregulation of rictor gene expression.

Conclusions: Here, we identify mTORC2 as a critical regulator of PVAT-directed protection of normal vascular tone. Modulation of mTORC2 activity in adipose tissue may be a potential therapeutic approach for inflammation-related vascular damage.

Keywords

mTORC2, perivascular adipose tissue, inflammation, inducible nitric oxide synthase, contractility

Introduction

Adipose tissue not only stores excess of energy as triacylglycerols but also secretes numerous growth factors, cytokines and hormones that are involved in overall energy homeostasis and metabolism.[1] During obesity, adipose tissue mass increases and dysfunction occurs favoring development of insulin resistance and cardiovascular disease.[1]

A crucial intracellular regulator of fatty acid metabolism and cell growth is the serine/ threonine kinase mammalian target of rapamycin (mTOR).[2] mTOR exists in two multi-protein complexes, mTOR complex 1 (mTORC1) and mTORC2.[3] The latter complex is characterized by its essential regulatory protein rictor and integrates signals from growth factors to regulate cell survival or cytoskeleton organization.[4-7] mTORC2 phosphorylates AGC kinase family members such as Akt at Serine 473.[8]

As full body knockout of rictor/ mTORC2 is embryonically lethal, [9] diverse tissue-specific knockout models of rictor have been generated to characterize the physiologic functions of rictor in the adult mouse.[4] Mice with specific ablation of rictor in adipose tissue have higher lean mass due to increased levels of insulin and insulin-like growth factor-1, display enhanced glucose metabolism and are insulin resistant.[10, 11]

Among the various and distinct adipose depots, perivascular adipose tissue (PVAT) not only serves as a structural support for most arteries but also secretes molecules to actively modulate vascular function.[12, 13] PVAT has an anticontractile function and this was shown for the first time in 1991 by Soltis and Cassis.[14] In 2002, Löhn et al. reported the release of a transferable vasoactive factor by PVAT that act on vascular smooth muscle cells (VSMCs) via ATP-dependent K^+ channels to mediate vasorelaxation.[15]

Since then, the list of dilatory or anticontractile molecules released from PVAT has expanded and now includes adipokines (e.g. adiponectin[16]), reactive oxygen species (e.g. hydrogen peroxide[17]) and others (e.g. methyl palmitate[18], hydrogen sulfide[19], and Angiotensin 1-7[20]). In 2005, Yudkin et al., proposed that obesity and its adverse effects causes PVAT to inflame, and to secrete tumor necrosis factor (TNF)α and interleukin (IL)6 which resulted in loss of PVAT's anticontractile function.[21] In rat mesenteric arteries, these inflammatory cytokines impaired the anticontractile activity of healthy PVAT,[22] and in mouse femoral arteries, endovascular injury upregulated inflammation in PVAT.[23]

Thus, the progression of the inflammatory reaction in PVAT appears to be crucial in altering PVAT's vasoactive properties, however, intracellular mechanisms that might control these reactions are not known. Recently, mTORC2-deficient mouse embryonic fibroblasts and rictor knockdown of dendritic cells exhibited a hyperinflammatory phenotype after lipopolysaccharide stimulation.[24] In this study, we have therefore tested the hypothesis that deletion of rictor in adipose tissue, and thereby inactivation of mTORC2 in PVAT, may modulate vascular function by increasing inflammation in PVAT.

Materials and Methods

Materials and Methods are available in the online-only Supplement.

Results

Adipose-Specific Deletion of Rictor Attenuates mTORC2 Signaling in Aortic PVAT

To analyze the role of mTORC2 in PVAT for vascular function, we used adipose cell-specific rictor knockout ($rictor^{ad-/-}$) and corresponding control ($rictor^{fl/fl}$) mice which were

described previously.[10] Adipose-specific rictor knockout was confirmed by significant reduction of rictor gene expression in epididymal fat (EFAT) from rictor$^{ad-/-}$ mice (Supplemental Figure I). Next, rictor gene expression in aorta (tissue containing mainly smooth muscle and endothelial cells) and in PVAT surrounding the thoracic aorta (referred henceforth as PVAT) was examined. The expression of rictor was significantly reduced in the PVAT but remained unchanged in the aorta from rictor$^{ad-/-}$ mice (Figure 1A). To evaluate mTORC2 activity, aortic rings with intact PVAT were stimulated with insulin. Subsequently, PVAT and aorta were separated and analyzed for Akt Ser473 phosphorylation, a known TORC2 substrate.[8] PVAT from rictor$^{ad-/-}$ mice exhibited reduced Akt Ser473 phosphorylation after insulin stimulation indicating impaired insulin signaling (Figure 1B, C). In the aorta, insulin-induced Akt Ser473 phosphorylation remained unchanged in the groups (Figure 1B, C). No difference was detected in insulin-stimulated phosphorylation of Erk1/2 between the mice groups in PVAT and aorta (Figure 1B).

Increased Aortic Contraction and Impaired Endothelium-Dependent Relaxation in Rictor$^{ad-/-}$ Mice in the Presence of PVAT

PVAT surrounding the arteries influences vascular function.[12, 13] To investigate whether PVAT from rictor$^{ad-/-}$ mice modulate aortic contractions, aortic rings with or without PVAT were used. To test the contractile capacity of the smooth muscle cell layer by direct depolarization, all rings were initially treated with100 mmol/L potassium chloride (KCl). In all rings, similar contractions independent of rictor and PVAT were observed (data not shown). Next, we investigated the contribution of rictor in PVAT to receptor-dependent vascular contraction. Aortic rings with or without PVAT were exposed to vasoconstrictor

phenylephrine (PE) in a concentration-dependent manner. Aortic rings with PVAT from rictor$^{ad-/-}$ mice displayed 2.1-fold higher maximal contractions as compared with rings from rictor$^{fl/fl}$ mice after treatment with PE (rictor$^{ad-/-}$: 43.2±6.3% vs. rictor$^{fl/fl}$: 20.1±3.8% at 3x10^{-6} mol/L, Figure 2A). With the removal of PVAT, contractions to PE increased overall and maximal contractions reached similar levels in both groups of mice (rictor$^{ad-/-}$: 70.0± 8.6% vs. rictor$^{fl/fl}$: 81.0±10.1% at 3x10^{-6} mol/L, Figure 2B). To determine whether vascular relaxation was also affected, we analyzed acetylcholine (ACh)-induced endothelium-dependent relaxation. ACh-induced relaxation in aortic rings with PVAT was impaired in rictor$^{ad-/-}$ mice (Figure 2C). This impairment was also confirmed by the pD_2 values, which suggests a delay in relaxation in rictor$^{ad-/-}$ aortic rings with PVAT (rictor$^{ad-/-}$: 6.2± 0.2 mol/L vs. rictor$^{fl/fl}$: 7.0±0.1 mol/L). Upon removal of PVAT, the differences were lost and the aortic rings relaxed normally (Figure 2D). As we found differences in contraction and dilation to receptor-dependent agonists in rings with PVAT, we further characterized contraction to KCl. Concentration-dependent (10 to 100 mmol/L) KCl-induced contractions in aortic rings with PVAT were similar between both groups of mice (Supplemental Figure II).

Hypothetically, increased aortic contraction with PVAT in rictor$^{ad-/-}$ mice might be due to reduced nitric oxide (NO) availability from endothelial nitric oxide synthase (eNOS). To investigate this L-NAME, which preferentially inhibits eNOS was used.[25] In the presence of L-NAME (300 µmol/L), the contractile responses to PE increased in rings with PVAT from both mice groups (Figure 2E). Nonetheless, PE-induced contractions were higher in aortic rings with PVAT from rictor$^{ad-/-}$ mice (1.5-fold; rictor$^{ad-/-}$: 86.36±8.17% vs. rictor$^{fl/fl}$: 58.78±6.71% at 3 x10^{-6} mol/L; Figure 2E).

To define the specificity of L-NAME for the different NO synthases we used RAW264.7 cell line which exclusively expresses inducible NOS, (iNOS/NOS2).[26] NO measurements after LPS stimulation revealed that L-NAME at 300 µmol/L also partially inhibited iNOS-induced NO production (approximately 40%, Supplemental Figure III). Expectedly, iNOS inhibitor 1400W, a highly specific and selective inhibitor [27], inhibited LPS-induced NO production to baseline levels (Supplementary Figure III).

In addition to NO, endothelium also releases other dilatory factors. Hence, experiments were performed with endothelium-denuded aortic rings with PVAT. Aortic contractions to PE or $PGF_{2\alpha}$ were significantly higher in rictor$^{ad-/-}$ mice compared with rictor$^{fl/fl}$ mice (Figure 2F and G). Taken together these results suggest that the anticontractile effect mediated by rictor is for the most part endothelium-independent.

Loss of Rictor in Adipose Cells of PVAT Results in Upregulation of Inflammatory Mediators

To determine how loss of rictor in adipose cells of PVAT increases aortic contractions and impairs relaxation, we screened genes which are expressed in and secreted by PVAT. These included adipokines[28], reactive oxygen species (ROS),[17, 29] and inflammatory molecules.[30] Amongst the adipokines, gene expression levels of adiponectin (adipoq) and lipocalin (lnc2) were not affected in the PVAT from rictor$^{ad-/-}$ mice (Figure 3A). However, the expression level of resistin (retn) was significantly reduced. Gene expression of NADPH oxidase subunits nox2, nox4, p22phox, and p67phox and adipocyte markers (PPARγ and FABP4) were not affected. Interestingly, the expression of inflammatory genes such as macrophage inflammatory protein 1α (Mip1α) and Tnfα were increased in the PVAT from rictor$^{ad-/-}$ mice (Figure 3A).

Protein analysis of conditioned media revealed increased release of IL-6 (5-fold), MIP1α (5-fold) and TNFα (4-fold) from PVAT of rictor$^{ad-/-}$ mice (Figure 3B).

Increased iNOS Expression in PVAT of Rictor $^{ad-/-}$ Mice

To investigate if the augmented expression of inflammatory molecules was associated with elevated macrophage infiltration in PVAT, we determined steady state mRNA expression levels of macrophage-associated genes emr1 (F4/80), CD163, and iNos. Expression of F4/80 and CD163 were similar between groups while iNos expression increased significantly in PVAT from rictor$^{ad-/-}$ mice (Figure 4A). To validate this, we examined in cross sections of thoracic aorta with PVAT the expression of iNOS. Indeed, iNOS expression was higher in the PVAT from rictor$^{ad-/-}$ mice (Figure 4B). The uniform expression of iNOS across the PVAT suggests that adipocytes themselves and not macrophages are the predominant cells expressing iNOS. Moreover, iNOS staining in aortic medial layer was hardly visible.

The percentages of macrophages and leukocytes in the vascular stromal fraction (SVF) were similar between groups in PVAT (Figure 4C). In EFAT, no differences in macropage and leukocyte percentages in SVF were detected, but overall percentages of macrophages and leukocytes were increased about 100% (Figure 4C).

Inhibition of iNOS Restores Anticontractile Effect of PVAT

TNFα stimulated iNos expression in 3T3-L1 adipocytes (Supplemental Figure IV) as reported previously.[31] To confirm our observation that iNOS is expressed mainly in PVAT (Figure 4B, only background staining in the medial layer of the aorta), we analyzed gene expression of iNos in aortic tissue and PVAT. Indeed, expression of iNos

was only detected in PVAT but not in the aorta of rictor$^{ad-/-}$ mice using quantitative real-time PCR (CT value in PVAT: 29; aorta: no amplification). Thus, we investigated the possible role of iNOS for vascular function using iNOS inhibitor 1400W.[27] In aortic rings with PVAT, contractions in rictor$^{ad-/-}$ mice were reduced in the presence of 1400W (Figure 5A) reaching similar levels detected in rictor$^{fl/fl}$ mice (Figure 5B). Additionally, treatment with 1400W improved the endothelium-dependent relaxation in aortic rings with PVAT from rictor$^{ad-/-}$ mice (Figure 5C) to comparable levels observed in control rings (Figure 5D). Thus, the altered function in aortic rings with PVAT in rictor$^{ad-/-}$ mice was normalized after inhibition of iNOS. Subsequently, we analyzed the effect of TNFα on PE-induced contractions, as this proinflammatory cytokine has been shown to counteract the anticontractile activity of PVAT.[22] In aortic rings with PVAT from rictor$^{fl/fl}$ mice, contractions to PE (10^{-6} mol/L) increased in the presence TNFα but not to a similar level as contractions in the rings from rictor$^{ad-/-}$ mice, which were significantly higher compared to untreated rings from rictor$^{fl/fl}$ mice (Supplemental Figure V). Thus, the increased contractility in rings with PVAT from rictor$^{ad-/-}$ mice might be partially also due to increased TNFα secreted from PVAT. Taken together, our findings suggest that iNOS in concert with TNFα and possibly other inflammation-associated molecules counteract the intrinsic anticontractile function in PVAT of rictor $^{ad-/-}$ mice.

Downregulation of Adipose Rictor Expression after High-Fat Diet Feeding

Since depletion of rictor in adipose tissue is associated with increased expression of inflammatory genes and proteins in PVAT, we assessed the possible physiological relevance of rictor expressional regulation after high-fat diet (HFD) feeding, a model of experimental obesity and chronic low grade inflammatory disease.[32]

We analyzed rictor gene expression levels in PVAT and EFAT in mice fed for 10-12 weeks with a HFD and with control diet (CD). Steady state mRNA expression levels of rictor were significantly downregulated in both types of adipose tissue after HFD (more than 30 %, Figure 6A, B; left panels). Concomitantly, iNos expression was significantly increased in PVAT of these HFD fed mice while in EFAT an upward trend was observed (P=0.16).

Discussion

In the present study, we describe a hitherto unknown function of the serine and threonine kinase complex mTORC2 controlling the anticontractile activity of PVAT primarily by regulating inflammation in the adipocytes. Downregulation of rictor, an essential mTORC2 component, in adipose tissue increased gene expression of Tnfα , Mip1α and iNos in PVAT and, concurrently increased the secretion of IL6, MIP1α and TNFα . Moreover, inhibition of iNOS restored the anticontractile activity of PVAT lacking rictor. Importantly, we demonstrate that in a model of low grade chronic inflammation, such as HFD-induced obesity, gene expression of rictor in PVAT is downregulated whereas that of iNOS is upregulated.

Studies addressing PVAT's contribution to vascular functions have largely focused on identifying molecules released by PVAT in normal and in pathological conditions such as obesity or hypertension.[13, 30] Signaling enzymes in PVAT that control these secretory molecules are not yet known. To the best of our knowledge, this is the first study to show the contribution of an intracellular molecule (rictor) in adipocytes of PVAT in regulating the anticontractile activity.

Jabs et al. have shown that continuous treatment with the mTOR inhibitor rapamycin, also known as sirolimus, markedly reduced vasorelaxation to ACh in rat aortae devoid of PVAT by inducing endothelial dysfunction associated with reduced nitric oxide (NO) availability.[33] Possible underlying mechanism may be inhibition of mTORC2 assembly in endothelial cells after long term rapamycin treatment[34] impairing downstream signaling from Akt to eNOS.[35, 36] In our study, depletion of rictor from adipose cells in PVAT increased aortic contractions in response to receptor-dependent vasoconstrictors and impaired vasorelaxation. Upon removing PVAT, the differences in contraction and dilation between the groups vanished supporting the current model stating that PVAT-released molecules directly mediate vasoactive effects.[13]

PVAT can exert its anticontractile effects via endothelium-dependent or -independent mechanisms.[17, 20] The endothelium-dependent effect involves release of NO from eNOS, which is required to maintain vascular tone, regulate platelet aggregation and leukocyte adhesion.[37] In our model, the anticontractile function of rictor was still present in rings with intact PVAT after eNOS inhibition or endothelium denudation. Thus, endothelial NO or other endothelium-derived vasodilators do not play a major role in rictor's anticontractile effects in PVAT. Inherent contractile responsiveness of vascular smooth muscle cells in the aortic rings was also preserved despite the loss of rictor in PVAT since KCl-induced contractions were identical. This suggests that mTORC2's anticontractile effects in PVAT are most likely due to modulation of the secretory protein profile affecting adjacent vascular cells without changing their inherent functionality. Increased inflammation and/ or oxidative stress in PVAT have been linked to promote vasoconstriction and endothelial dysfunction.[38, 39] In this regard, we screened the expression of reactive oxygen species generating NADPH oxidases and inflammatory

cytokines. In PVAT lacking rictor, expression of only inflammatory cytokines was increased. Thus, in murine PVAT, decreased mTORC2 activity turned on a cascade of inflammatory pathways.

Vascular expression of iNOS occurs during pathologic changes in the vascular wall such as atherosclerosis development, hypertension and vascular injury.[40] These pathologies are often associated with inflammatory processes which induce expression of iNOS in the vascular wall. Healthy blood vessels do not express iNOS.[41] Consistent with this finding, we did not detect iNOS expression in thoracic arterial tissue, i.e. endothelium plus VSMCs, without PVAT. Tian and co-workers have demonstrated that inhibition of iNOS protects endothelium/NO-dependent vasodilation of thoracic aorta in aged rats.[42] Vice versa, overexpression of iNOS using gene transfer resulted in impaired NO-dependent vasorelaxation in carotid arteries.[43] In our work, specific inhibition of iNOS with 1400W protected vasodilation and restored anticontractile activity in PVAT lacking rictor. Even though L-NAME inhibited iNOS by 40% still the contractions were higher in rings with PVAT lacking rictor. This suggests that partial inhibition of iNOS is not enough to restore anticontractile activity in PVAT.

Why removal of PVAT expressing iNOS increase and not reduce contraction? As explanation, we propose that the PVAT, expressing iNOS, also secretes anticontractile molecules acting on the smooth muscle cell layer. The release of procontractile molecules counteract but can't abolish the overall anticontractile function, which is ultimately lost only after removal of PVAT

The marked reduction in insulin-stimulated Akt phosphorylation in PVAT of rictor $^{ad-/-}$ mice may not only be caused by reduced mTORC2 to Akt signaling but may also be attributed to insulin resistance in these mice,[10, 11] resulting in impaired insulin signaling

already at the level of the insulin receptor substrates.[44] Brown and coworker have demonstrated that expression of a constitutively active Akt variant normalizes the hyperinflammatory phenotype in rictor-deficient cells by restoring mTORC2 downstream signaling.[24] Thus, these increased inflammatory expression profiles, in our study, possibly may be caused by defective Akt signaling in PVAT lacking rictor.

Infiltration of macrophages and T-cells in PVAT has been reported in mice fed with high-fat diet.[28, 30] In contrast, thoracic PVAT has also been reported to be relatively resistant to macrophage infiltration, to obesity-induced inflammation and is nearly identical to interscapular brown adipose tissue.[45] In our study, when we compared the stromal vascular fractions of PVAT and EFAT from mice, we found about half as much leukocytes and macrophages in PVAT as compared with EFAT. This observation argues against an intrinsically pro-inflammatory depot in PVAT. Moreover, there was no difference in macrophage presence in PVAT between rictor$^{fl/fl}$ and rictor$^{ad-/-}$ mice. Thus, we suggest that ablation of rictor in adipocytes provide and promote a complementary source for propagation of inflammation.

Obesity promotes inflammation in PVAT of thoracic aorta and in PVAT of other parts of the arterial tree.[22, 46, 47] Increased expression of inflammatory cytokines such as TNFα and IL6 in PVAT of obese patients has been implicated to reduce its anticontractile activity.[22] Intriguingly, in our model, experimental obesity induced via high-fat diet feeding per se downregulated gene expression of rictor in thoracic PVAT while iNos expression was upregulated. Moreover, rictor deletion promoted a hyper-inflammatory phenotype in PVAT that resembles obesity-induced changes. We speculate that inflammation, possibly TNFα induces a series of signaling cascades in perivascular adipocytes resulting in downregulation of rictor expression. Furthermore, reduced

mTORC2 assembly and signaling in turn might further advance the ongoing inflammatory response.

In conclusion, the present findings assign a decisive function to rictor in PVAT in protecting arteries from inflammatory stress and in controlling normal vascular function. Stabilizing expression of rictor in adipose tissue during obesity and other metabolic rearrangements might therefore embody a novel treatment approach to combat inflammation-associated vascular damage.

Acknowledgements

We thank Ana Perez-Dominguez and Emerita Ammann Meier for their expert technical assistance.

Sources of Funding

This work was supported by funding from University of Zurich, University Hospital of Zurich, and Swiss National Science Foundation.

Disclosures

None.

References

1. Hajer GR, van Haeften TW, Visseren FL. Adipose tissue dysfunction in obesity, diabetes, and vascular diseases. *Eur Heart J*. 2008;29:2959-2971
2. Soliman GA. The integral role of mtor in lipid metabolism. *Cell Cycle*. 2011;10:861-862
3. Loewith R, Jacinto E, Wullschleger S, Lorberg A, Crespo JL, Bonenfant D, Oppliger W, Jenoe P, Hall MN. Two tor complexes, only one of which is rapamycin sensitive, have distinct roles in cell growth control. *Mol Cell*. 2002;10:457-468
4. Oh WJ, Jacinto E. Mtor complex 2 signaling and functions. *Cell Cycle*. 2011;10:2305-2316
5. Cybulski N, Hall MN. Tor complex 2: A signaling pathway of its own. *Trends Biochem Sci*. 2009;34:620-627

6. Sarbassov DD, Ali SM, Kim DH, Guertin DA, Latek RR, Erdjument-Bromage H, Tempst P, Sabatini DM. Rictor, a novel binding partner of mtor, defines a rapamycin-insensitive and raptor-independent pathway that regulates the cytoskeleton. *Curr Biol*. 2004;14:1296-1302
7. Jacinto E, Loewith R, Schmidt A, Lin S, Ruegg MA, Hall A, Hall MN. Mammalian tor complex 2 controls the actin cytoskeleton and is rapamycin insensitive. *Nat Cell Biol*. 2004;6:1122-1128
8. Sarbassov DD, Guertin DA, Ali SM, Sabatini DM. Phosphorylation and regulation of akt/pkb by the rictor-mtor complex. *Science*. 2005;307:1098-1101
9. Shiota C, Woo JT, Lindner J, Shelton KD, Magnuson MA. Multiallelic disruption of the rictor gene in mice reveals that mtor complex 2 is essential for fetal growth and viability. *Dev Cell*. 2006;11:583-589
10. Cybulski N, Polak P, Auwerx J, Ruegg MA, Hall MN. Mtor complex 2 in adipose tissue negatively controls whole-body growth. *Proc Natl Acad Sci U S A*. 2009;106:9902-9907
11. Kumar A, Lawrence JC, Jr., Jung DY, Ko HJ, Keller SR, Kim JK, Magnuson MA, Harris TE. Fat cell-specific ablation of rictor in mice impairs insulin-regulated fat cell and whole-body glucose and lipid metabolism. *Diabetes*. 2010;59:1397-1406
12. Aghamohammadzadeh R, Withers S, Lynch F, Greenstein A, Malik R, Heagerty A. Perivascular adipose tissue from human systemic and coronary vessels: The emergence of a new pharmacotherapeutic target. *Br J Pharmacol*. 2012;165:670-682
13. Szasz T, Webb RC. Perivascular adipose tissue: More than just structural support. *Clin Sci (Lond)*. 2012;122:1-12
14. Soltis EE, Cassis LA. Influence of perivascular adipose tissue on rat aortic smooth muscle responsiveness. *Clin Exp Hypertens A*. 1991;13:277-296
15. Lohn M, Dubrovska G, Lauterbach B, Luft FC, Gollasch M, Sharma AM. Periadventitial fat releases a vascular relaxing factor. *FASEB J*. 2002;16:1057-1063
16. Fesus G, Dubrovska G, Gorzelniak K, Kluge R, Huang Y, Luft FC, Gollasch M. Adiponectin is a novel humoral vasodilator. *Cardiovasc Res*. 2007;75:719-727
17. Gao YJ, Lu C, Su LY, Sharma AM, Lee RM. Modulation of vascular function by perivascular adipose tissue: The role of endothelium and hydrogen peroxide. *Br J Pharmacol*. 2007;151:323-331
18. Lee YC, Chang HH, Chiang CL, Liu CH, Yeh JI, Chen MF, Chen PY, Kuo JS, Lee TJ. Role of perivascular adipose tissue-derived methyl palmitate in vascular tone regulation and pathogenesis of hypertension. *Circulation*. 2011;124:1160-1171
19. Kohn C, Schleifenbaum J, Szijarto IA, Marko L, Dubrovska G, Huang Y, Gollasch M. Differential effects of cystathionine-gamma-lyase-dependent vasodilatory h2s in periadventitial vasoregulation of rat and mouse aortas. *PLoS One*. 2012;7:e41951
20. Lee RM, Lu C, Su LY, Gao YJ. Endothelium-dependent relaxation factor released by perivascular adipose tissue. *J Hypertens*. 2009;27:782-790
21. Yudkin JS, Eringa E, Stehouwer CD. "Vasocrine" signalling from perivascular fat: A mechanism linking insulin resistance to vascular disease. *Lancet*. 2005;365:1817-1820
22. Greenstein AS, Khavandi K, Withers SB, Sonoyama K, Clancy O, Jeziorska M, Laing I, Yates AP, Pemberton PW, Malik RA, Heagerty AM. Local inflammation and hypoxia abolish the protective anticontractile properties of perivascular fat in obese patients. *Circulation*. 2009;119:1661-1670
23. Takaoka M, Suzuki H, Shioda S, Sekikawa K, Saito Y, Nagai R, Sata M. Endovascular injury induces rapid phenotypic changes in perivascular adipose tissue. *Arterioscler Thromb Vasc Biol*. 2010;30:1576-1582
24. Brown J, Wang H, Suttles J, Graves DT, Martin M. Mammalian target of rapamycin complex 2 (mtorc2) negatively regulates toll-like receptor 4-mediated inflammatory response via foxo1. *J Biol Chem*. 2011;286:44295-44305
25. Luo Z, Fujio Y, Kureishi Y, Rudic RD, Daumerie G, Fulton D, Sessa WC, Walsh K. Acute modulation of endothelial akt/pkb activity alters nitric oxide-dependent vasomotor activity in vivo. *J Clin Invest*. 2000;106:493-499
26. Naureckiene S, Edris W, Ajit SK, Katz AH, Sreekumar K, Rogers KE, Kennedy JD, Jones PG. Use of a murine cell line for identification of human nitric oxide synthase inhibitors. *J Pharmacol Toxicol Methods*. 2007;55:303-313
27. Garvey EP, Oplinger JA, Furfine ES, Kiff RJ, Laszlo F, Whittle BJ, Knowles RG. 1400w is a slow, tight binding, and highly selective inhibitor of inducible nitric-oxide synthase in vitro and in vivo. *J Biol Chem*. 1997;272:4959-4963

28. Takaoka M, Nagata D, Kihara S, Shimomura I, Kimura Y, Tabata Y, Saito Y, Nagai R, Sata M. Periadventitial adipose tissue plays a critical role in vascular remodeling. *Circ Res*. 2009;105:906-911
29. Gao YJ, Takemori K, Su LY, An WS, Lu C, Sharma AM, Lee RM. Perivascular adipose tissue promotes vasoconstriction: The role of superoxide anion. *Cardiovasc Res*. 2006;71:363-373
30. Chatterjee TK, Stoll LL, Denning GM, Harrelson A, Blomkalns AL, Idelman G, Rothenberg FG, Neltner B, Romig-Martin SA, Dickson EW, Rudich S, Weintraub NL. Proinflammatory phenotype of perivascular adipocytes: Influence of high-fat feeding. *Circ Res*. 2009;104:541-549
31. Juan CC, Lien CC, Chang CL, Huang YH, Ho LT. Involvement of inos and no in tnf-alpha-downregulated resistin gene expression in 3t3-l1 adipocytes. *Obesity (Silver Spring)*. 2008;16:1219-1225
32. Hassan M, Latif N, Yacoub M. Adipose tissue: Friend or foe? *Nat Rev Cardiol*. 2012;9:689-702
33. Jabs A, Gobel S, Wenzel P, Kleschyov AL, Hortmann M, Oelze M, Daiber A, Munzel T. Sirolimus-induced vascular dysfunction. Increased mitochondrial and nicotinamide adenosine dinucleotide phosphate oxidase-dependent superoxide production and decreased vascular nitric oxide formation. *J Am Coll Cardiol*. 2008;51:2130-2138
34. Sarbassov DD, Ali SM, Sengupta S, Sheen JH, Hsu PP, Bagley AF, Markhard AL, Sabatini DM. Prolonged rapamycin treatment inhibits mtorc2 assembly and akt/pkb. *Mol Cell*. 2006;22:159-168
35. Dimmeler S, Fleming I, Fisslthaler B, Hermann C, Busse R, Zeiher AM. Activation of nitric oxide synthase in endothelial cells by akt-dependent phosphorylation. *Nature*. 1999;399:601-605
36. Fulton D, Gratton JP, McCabe TJ, Fontana J, Fujio Y, Walsh K, Franke TF, Papapetropoulos A, Sessa WC. Regulation of endothelium-derived nitric oxide production by the protein kinase akt. *Nature*. 1999;399:597-601
37. Kubes P, Suzuki M, Granger DN. Nitric oxide: An endogenous modulator of leukocyte adhesion. *Proc Natl Acad Sci U S A*. 1991;88:4651-4655
38. Withers SB, Agabiti-Rosei C, Livingstone DM, Little MC, Aslam R, Malik RA, Heagerty AM. Macrophage activation is responsible for loss of anticontractile function in inflamed perivascular fat. *Arterioscler Thromb Vasc Biol*. 2011;31:908-913
39. Ketonen J, Shi J, Martonen E, Mervaala E. Periadventitial adipose tissue promotes endothelial dysfunction via oxidative stress in diet-induced obese c57bl/6 mice. *Circ J*. 2010;74:1479-1487
40. Ginnan R, Guikema BJ, Halligan KE, Singer HA, Jourd'heuil D. Regulation of smooth muscle by inducible nitric oxide synthase and nadph oxidase in vascular proliferative diseases. *Free Radic Biol Med*. 2008;44:1232-1245
41. Wilcox JN, Subramanian RR, Sundell CL, Tracey WR, Pollock JS, Harrison DG, Marsden PA. Expression of multiple isoforms of nitric oxide synthase in normal and atherosclerotic vessels. *Arterioscler Thromb Vasc Biol*. 1997;17:2479-2488
42. Tian J, Yan Z, Wu Y, Zhang SL, Wang K, Ma XR, Guo L, Wang J, Zuo L, Liu JY, Quan L, Liu HR. Inhibition of inos protects endothelial-dependent vasodilation in aged rats. *Acta Pharmacol Sin*. 2010;31:1324-1328
43. Gunnett CA, Lund DD, Chu Y, Brooks RM, 2nd, Faraci FM, Heistad DD. No-dependent vasorelaxation is impaired after gene transfer of inducible no-synthase. *Arterioscler Thromb Vasc Biol*. 2001;21:1281-1287
44. Boura-Halfon S, Zick Y. Phosphorylation of irs proteins, insulin action, and insulin resistance. *Am J Physiol Endocrinol Metab*. 2009;296:E581-591
45. Fitzgibbons TP, Kogan S, Aouadi M, Hendricks GM, Straubhaar J, Czech MP. Similarity of mouse perivascular and brown adipose tissues and their resistance to diet-induced inflammation. *Am J Physiol Heart Circ Physiol*. 2011;301:H1425-1437
46. Police SB, Thatcher SE, Charnigo R, Daugherty A, Cassis LA. Obesity promotes inflammation in periaortic adipose tissue and angiotensin ii-induced abdominal aortic aneurysm formation. *Arterioscler Thromb Vasc Biol*. 2009;29:1458-1464
47. Marchesi C, Ebrahimian T, Angulo O, Paradis P, Schiffrin EL. Endothelial nitric oxide synthase uncoupling and perivascular adipose oxidative stress and inflammation contribute to vascular dysfunction in a rodent model of metabolic syndrome. *Hypertension*. 2009;54:1384-1392

Significance

Perivascular adipose tissue (PVAT) surrounds most arteries and has anticontractile function. Increased inflammation in the vasculature associated PVAT is present during hypertension, atherosclerosis and obesity. Our study reveals a yet unexplored function of rictor, an essential component of mTOR complex 2, in perivascular adipocytes to regulate anticontractility via inhibiting the expression of inflammatory cytokines and iNOS. Our results suggest a direct gate keeper function for perivascular adipose mTORC2 in mediating vascular inflammation. The present findings underscore the importance to address mTORC2 signaling during inflammation-induced vascular damage.

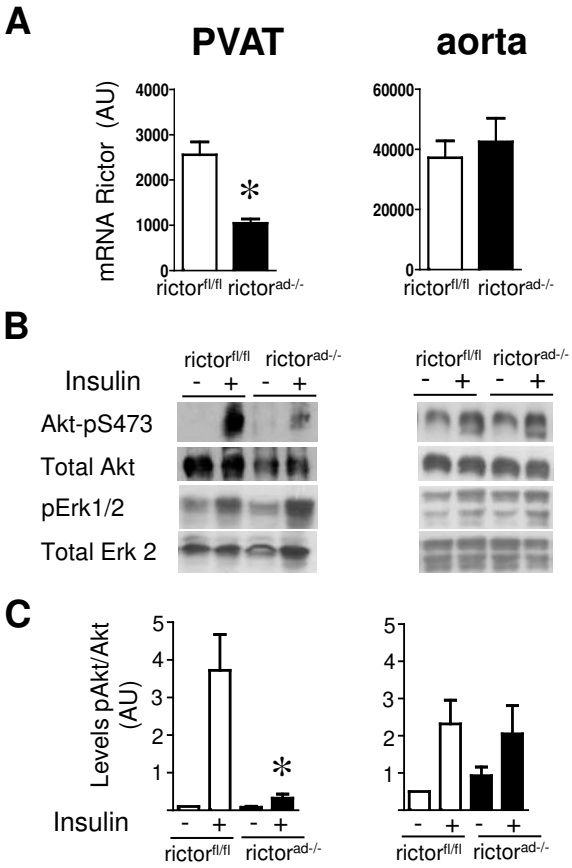

Figure 1. Adipose cell-specific deletion of rictor results in decreased expression of rictor and reduced Akt phosphorylation in PVAT. (**A**) Steady state mRNA expression levels of rictor in PVAT (n=9/10) and aortic tissue (n=4) were determined in rictor$^{fl/fl}$ and rictor$^{ad-/-}$ mice using quantitative real-time PCR. (**B)** Immunoblot analysis of insulin-stimulated phosphorylation of Akt at Ser473 and Erk1/2 in PVAT and aorta from rictor$^{fl/fl}$ and rictor$^{ad-/-}$ mice. Total Akt and Erk2 were used to control for protein loading. One representative blot out of three is shown. (**C**) Quantification of pAkt in PVAT and aorta from rictor$^{fl/fl}$ and rictor$^{ad-/-}$ mice (n=3). Densitometric analysis was first normalized to total Akt and then to untreated rictor$^{fl/fl}$. All data represent means ± SEM. *P<0.05 vs. rictor $^{fl/fl}$.

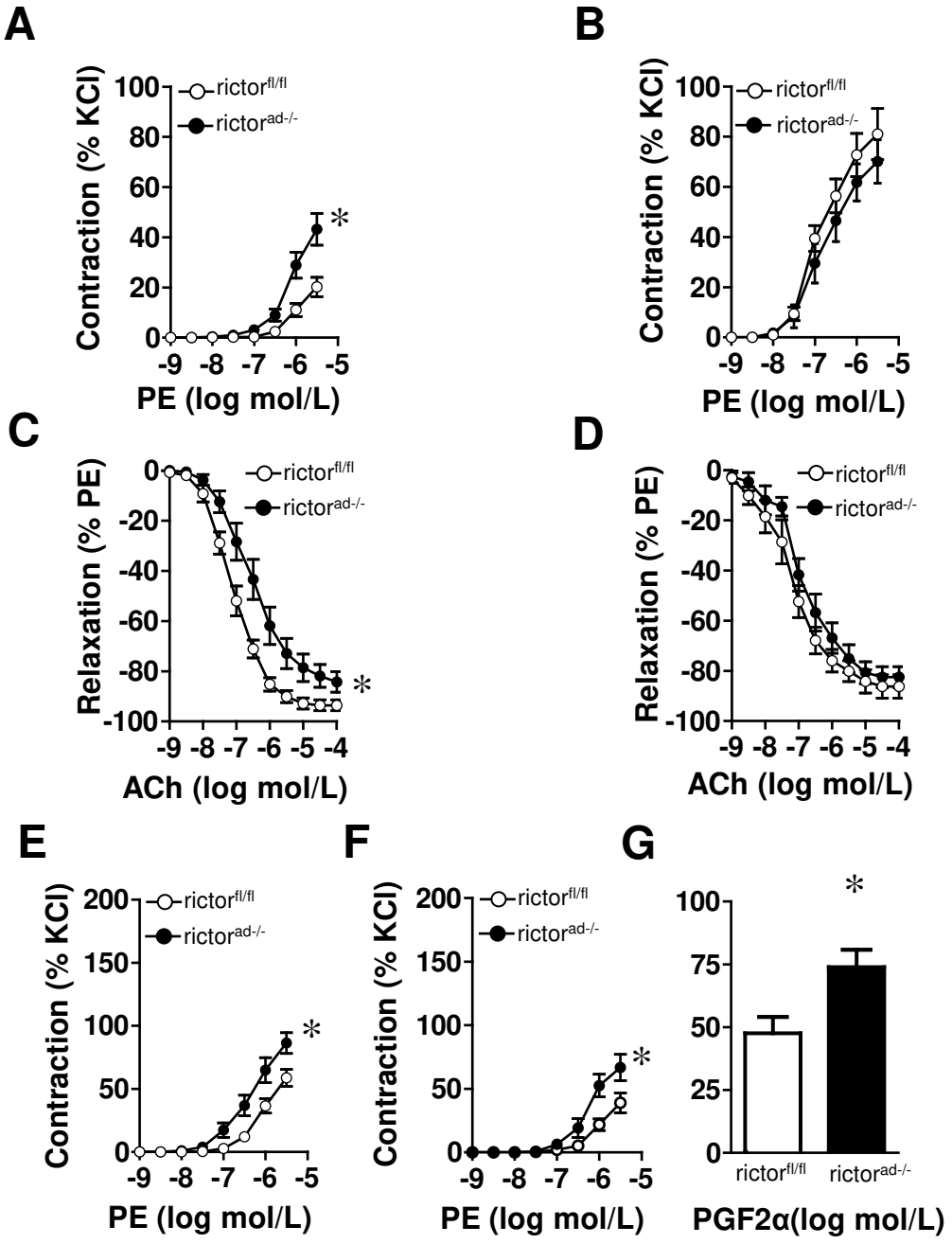

Figure 2. Rictor controls anticontractility in PVAT. Aortic rings from rictor$^{fl/fl}$ and rictor$^{ad-/-}$ mice were used. Rings with PVAT (**A**) or without PVAT (**B**) were contracted with PE (10^{-9} – $3x10^{-6}$ mol/L) in a concentration-dependent manner (n=10-13). Rings with PVAT (**C**) or without PVAT (**D**) were pre-contracted with PE and treated with Ach (10^{-9} – $3x10^{-6}$ mol/L) in a concentration-dependent manner (n=7-13). (**E**) Aortic rings with PVAT were pre-treated with L-NAME (300 $x10^{-6}$ mol/L) and then contracted with PE in a concentration-dependent manner (n=5-13). (**F** and **G)** Aortic rings with PVAT but without endothelium were treated in a concentration-dependent manner with PE or with $3x10^{-6}$ mol/L of $PGF_{2\alpha}$ (n=6-9). All Values are means±SEM. **P*<0.05 vs. rictor$^{fl/fl}$

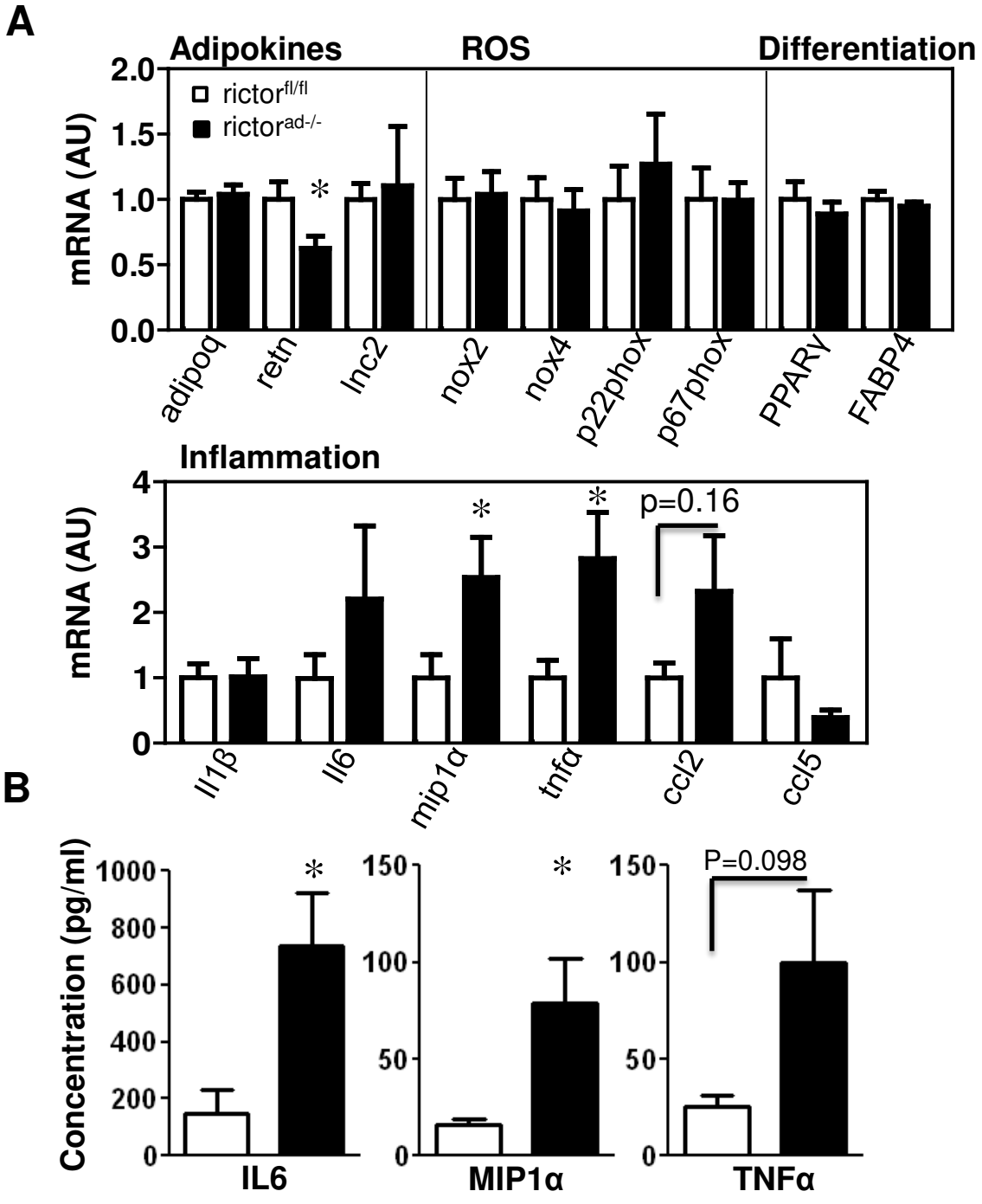

Figure 3. Adipocyte-specific deletion of rictor increases expression of inflammatory molecules in PVAT. (**A**) Steady state mRNA expression levels of adipokines, ROS, adipocyte differentiation and inflammatory molecules as determined by quantitative real-time PCR. Results are normalized to the levels in PVAT from rictor$^{fl/fl}$ mice (n=4-8). (**B**) Protein concentrations of inflammatory cytokines released by PVAT were determined in conditioned media using Bioplex system (n=4). All values represent means ± SEM, **P*<0.05 vs. rictor$^{fl/fl}$.

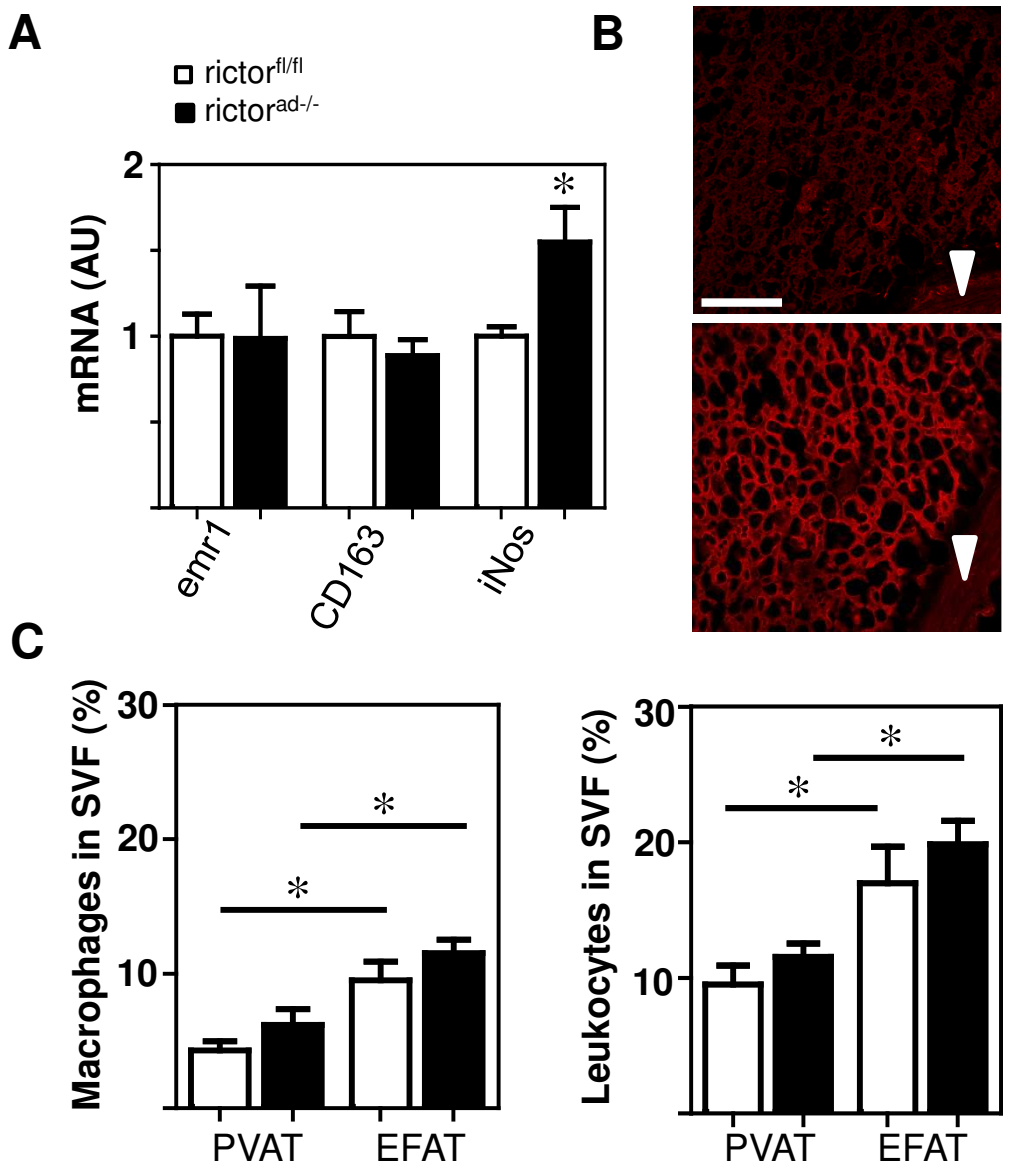

Figure 4. Elevated iNOS expression in PVAT from rictor$^{ad\ -/-}$ mice is independent of macrophage infiltration. (**A)** Steady state mRNA expression levels of emr (F4/80), CD163, and iNos were determined by quantitative real-time PCR. Results are normalized to the levels in PVAT from rictor$^{fl/fl}$ mice (n=8-14), **P*<0.05 vs. rictor$^{fl/fl}$. (**B)** immunofluorescence staining of iNOS (red) in cross sections of thoracic aorta with PVAT from rictor$^{fl/fl}$ (upper panel) and rictor$^{ad-/-}$ (lower panel) mice. Arrow heads indicate medial layer. Scale bar, 100 µm. Images are representative of n≥3 mice. (**C**), Percentages of macrophages (F4/80 and CD45.2 positive cells) and leukocytes (CD45.2 positive cells) in SVF from PVAT and EFAT using flow cytometry, data are means ± SEM, n=4-5, **P*<0.05 . All values represent means ± SEM.

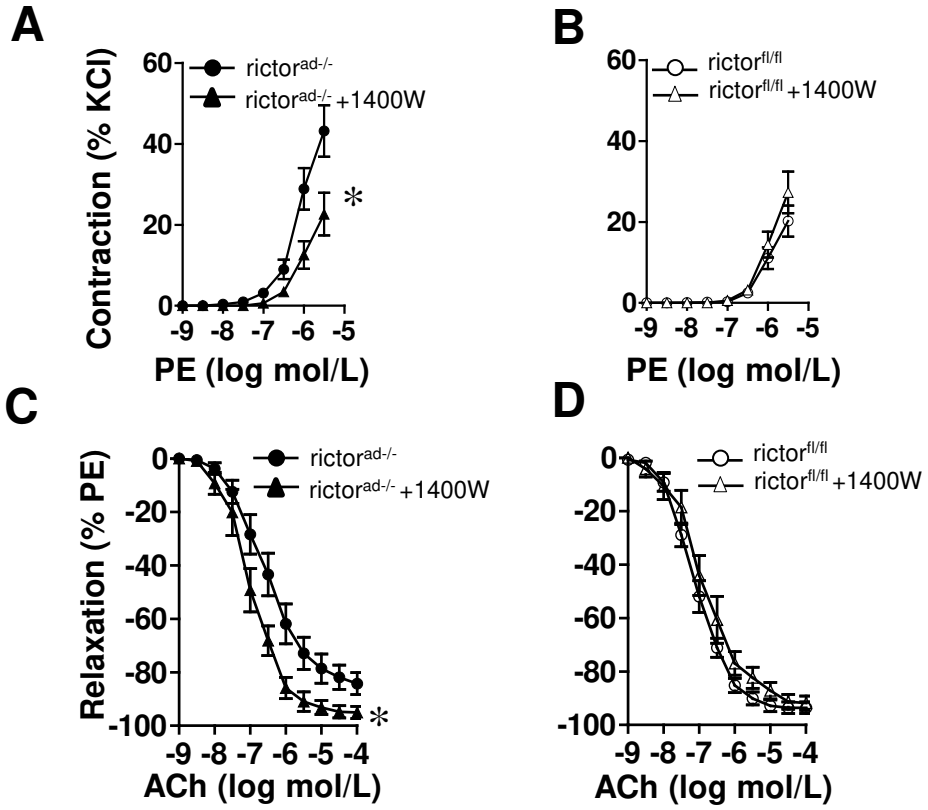

Figure 5. Inhibition of iNOS in PVAT normalizes vascular reactivity in rictor$^{ad-/-}$ mice. (**A** and **B**) Aortic rings with PVAT from rictor$^{ad-/-}$ and rictor$^{fl/fl}$ mice were contracted with PE in the presence or absence of iNOS inhibitor 1400W. rictor$^{ad-/-}$ pD2: 5.4±0.2 mol/L vs. rictor$^{ad-/-}$ +1400W pD2: 4.8±0.2 mol/L (n=11-13) **P*<0.05 vs. rictor$^{ad-/-}$ by pD2. (**C** and **D**) Precontracted aortic rings with PVAT were relaxed using ACh in the presence or absence of 1400W (n=7-13), **P*<0.05 vs. rictor$^{ad-/-}$. All values are means±SEM..

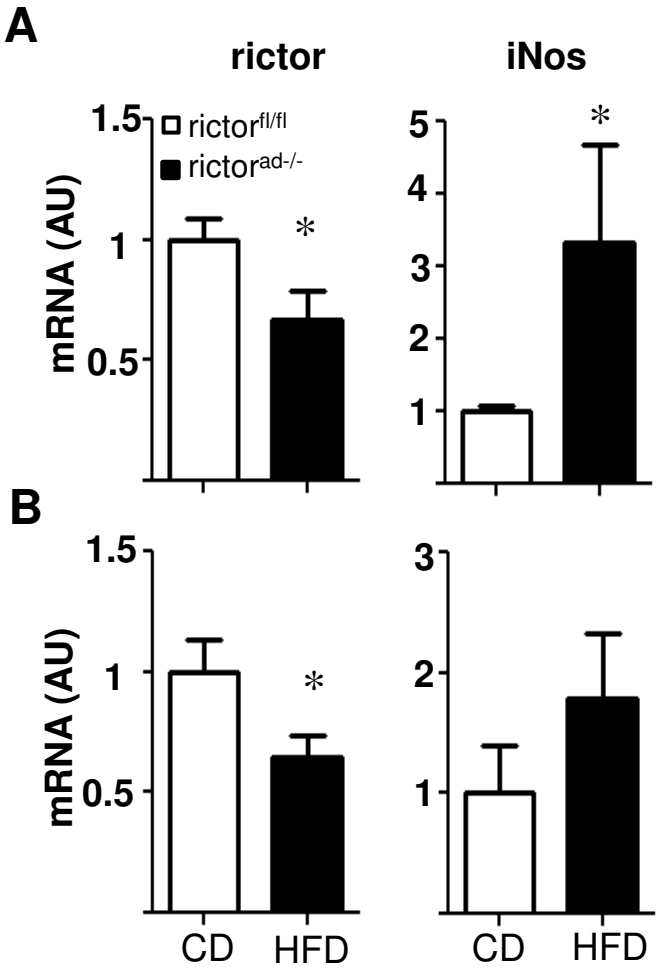

Figure 6. Differential effects of high-fat diet feeding on expression of rictor and iNOS in different fat depots. Steady state mRNA expression levels of rictor and iNos in PVAT (**A**) and EFAT (**B**) of mice fed with control diet (CD, n=5-9) or high-fat diet (HFD, n=6-9). Results are normalized to the levels from mice fed CD. Values are means±SEM. **P*<0.05 vs. CD.

Online Supplementary

Materials and Methods

Mice

The mice used in the present study were described before in detail.[1] Briefly, mice with adipose-specific deletion of rictor (*rictor*$^{ad-/-}$) were generated by crossing *rictor*$^{fl/fl}$ mice with C57BL/6J mice expressing Cre recombinase under the control of the adipocyte-specific *fabp4*/*aP2* gene promoter (purchased from JAX Laboratories, Bar Harbor, Maine, USA). Male mice (5 months) were used for all experiments which were backcrossed at least 5 times with the C57BL/6J strain except for flow cytometry analysis for which female mice (5-6 months) were used. Littermates with the *lox*/*lox* genotype (*rictor*$^{fl/fl}$) were used as control group in all experiments. Mice were housed at the institutional animal facilities (University Hospital Zurich and Biozentrum Basel, Switzerland, respectively) with a 12 hour light/dark cycle. Animals had access to standard chow (4.5% calories from fat; Kliba Nafag, Kaiseraugust, Switzerland) and to water *ad libitum*. Another group of male mice 8 weeks of age were fed high-fat diet (60% calories from fat; Harlan Research Diets) for 10-12 weeks. All mice used were genotyped with specific primers using PCR and standard protocols. Before sacrifice, mice were weighed and anesthetized by i.p. injection (xylazine: 100; ketamine: 23; and acepromazine: 3.0; in mg/kg body weight) and exsanguinated via cardiac puncture. Mice used for vascular function and insulin stimulation experiments were starved overnight. All mouse experiments described here were approved by the Kantonales Veterinaeramt of Basel-Stadt and Zurich, Switzerland, respectively.

Cell Culture

3T3-L1 cells were cultured in DMEM medium (Biochrome AG, Berlin, Germany) supplemented with 10% FCS and differentiated to adipocytes as described.[2] Briefly, post-confluent 3T3-L1 cells were treated with 3-isobutyl-1-methylxanthine (500 µM), dexamethasone (0.25 µM), insulin (10 µg/ml) and rosiglitazone (2 µM) for 2 days. Thereafter, cells were treated with insulin (1 µg/ml) for next 2 days. The cells were then maintained in DMEM medium with 10% FCS for 6 additional days and the media was changed every 2nd day. Differentiated adipocytes were kept overnight in DMEM medium with 0.5% FCS and then stimulated without or with TNFα (10 ng/ml) for 24 h. RAW264.7 cells were cultured in DMEM medium with 10% FCS.

Nitric Oxide Measurement

Nitric oxide is converted to nitrate and nitrite in the cell and is released in the conditioned media. RAW264.7 cells were treated with lipopolysaccharide for 24h in the absence or in the

presence of L-NAME (300 µM) or 1400W (1µM). In the conditioned media, nitrite concentrations were determined using Griess reagent (Sigma-Aldrich Chemie GmbH, Buchs, Switzerland) and optical density was measured at 540 nm. The amount of nitrite in the culture media was quantified using sodium nitrite as a reference standard.

RNA Isolation and Quantitative PCR

RNA isolation, cDNA preparation and real-time quantitative PCR were performed from epididymal fat, thoracic PVAT and aortae using standard protocols. Briefly, RNA from fat tissues was extracted using RNeasy lipid tissue mini kit and from aorta using RNeasy fibrous tissue kit according to the protocol of the manufacturer (Qiagen, Hombrechtikon, Switzerland). Total RNA was transcribed into cDNA using WT (Whole Transcript)-Ovation™ Pico RNA Amplification System from NuGEN (Bemmel, Netherlands). Quantitative real-timepolymerase chain reaction (qRT-PCR) was performed using specifically designed mouse primer pairs for the genes analyzed in the present study (Table S1). Gene expression in epididymal fat and PVAT was normalized to acidic ribosomal phosphoprotein (Arbp) and in aortic tissue to β-actin using the comparative C(T) method.[3]

Vascular Function Analysis

Experiments were performed as described before.[4, 5] After sacrifice, thoracic aorta was dissected, placed in cold (4°C) Krebs-Ringer bicarbonate solution (in mmol/l: NaCl 118.6; KCl 4.7; $CaCl_2$ 2.5;$MgSO_4$ 1.2; KH_2PO_4 1.2; $NaHCO_3$ 25.1; $EDTA_{Na2Ca}$ 0.026; glucose 10.1). To check the effect of PVAT on vascular function, aorta was either cleaned of adhering PVAT or was left intact. Aorta with or without fat was cut into equal-sized rings (2.5 mm of length) under a dissection microscope (Olympus SZX9, Volketswil, Switzerland), and care was taken not to damage the endothelium during preparation. Rings were mounted on tungsten wires (100 µm in diameter) and placed vertically in water-jacketed organ chambers containing 10 ml of Krebs buffer maintained at 37°C and pH 7.4 with constant gassing (95% O_2 and 5% CO_2). One end of each wire was fixed to a stainless steel rod, and the other end was connected to force transducers (Hugo Sachs Electronik, March-Hugstetten, Germany). Rings were stretched in a stepwise manner until a resting tension of 3.5 g was achieved. Stretched rings were allowed to equilibrate for 30 min before exposing with KCl (100 mmol/L) until a stable contractile response was reached. The rings were exposed to phenylephrine (PE; 10^{-9}- $3x10^{-6}$ mol/L), prostaglandin$_{2\alpha}$ ($PGF_{2\alpha}$; 10^{-6}- $3x10^{-6}$ mol/L) or acetylcholine (ACh; 10^{-9}-10^{-4} mol/L) in a concentration-dependent manner. To block nitric oxide synthase (NOS) selected aortic rings were treated with either N^G-nitro-L-arginine methyl ester (L-NAME; $300x10^{-6}$ mol/l) [4] or with iNOS inhibitor (1400 W, 10^{-6} mol/L).[6]

To check the vascular smooth muscle cells-dependent contractile responses, aortic rings with PVAT were exposed to increasing concentration of KCl (10 to 100 mmol/L).
For endothelial denudation experiments, selected rings were exposed for 10 sec to 1% Triton X-100 before mounting into the organ chamber. Endothelial denudation was tested by treating PE -precontracted rings with ACh followed by treatment with sodium nitroprusside (10^{-5} mol/L), a nitric oxide donor.

Insulin stimulation and Immunoblotting

Aortic rings with PVAT were mounted to organ chambers and stretched as described above. After 30 min of equilibration, tissues were stimulated with insulin (1µmol/L). After 10 min, tissues were transferred into ice cold Krebs Ringer buffer and PVAT was separated from the aortic tissue. Both tissues (PVAT or aorta without PVAT) were homogenized using Qiagen tissue lyser in lysis buffer containing Tris.Cl (50 mmol/L, pH 7.4), NaCl (150 mmol/L), EDTA (1 mmol/L), NP-40 (1%), protease inhibitor, and phosphatase inhibitor cocktail (Sigma, Buchs, Switzerland). Equal amounts of protein were loaded for SDS-PAGE, transferred to nitrocellulose and analyzed with the indicated antibodies. Immunoblotting was performed using the antibodies against phospho Akt (pSer473), Akt and phospho Erk1/2 (Cell Signaling, Danver, MA, USA) and ERK2 (Santa Cruz Biotechnology, Santa Cruz, CA, USA) and corresponding HRP-conjugated secondary antibodies (GE Healthcare, Buckinghamshire, UK). Labeled proteins were visualized on X-ray films using a chemiluminescence reaction. Quantification of blots was performed by using the software ImageJ 1.40g (NIH, USA).

Bioplex Assay

Thoracic aortic PVAT was excised and incubated in a 96- well plate containing 200µl Phenol Red-free and serum-free DMEM/Ham's F-12 medium (BioConcept Amimed, Allschwill, Switzerland) for 48h. Conditioned media was collected, shock-frozen in liquid nitrogen and stored at -80°C. Concentrations of MIP-1α, TNFα and IL-6 levels in the conditioned media were determined using BioPlex Pro Mouse cytokine Group 1 (customized 3-plex assay, BioRad, Hercules CA, USA) according to the recommendations of the manufacturer. Data were analyzed using the BioPlex Manager 4.1.1 software. Cytokine concentration in PVAT was quantified based on Logistic-5PL regression standard curve. Values were normalized to protein content in the conditioned media.

Immunofluorescence analysis of cryosectios

Thoracic aortae with PVAT from *rictor*$^{ad-/-}$ and *rictor*$^{fl/fl}$ mice were embedded in Tissue Tec (Sakura, Germany) and stored at –80°C. Cross sections (10 µm) were cut using a cryostat and mounted on superfrost plus slides (Thermo Fisher, Germany). Slides were used directly for immunofluorescence analysis or stored at - 80°C until needed. Before staining, slides were dried at room temperature (RT) for 20 minutes and fixed with 4 % PFA in PBS (pH 7.4) for 10 minutes. Slides were washed twice for 5 minutes in PBS (pH 7.4). Sections were incubated in blocking buffer (0.1% Tween 20, 5% goat serum in PBS) for 60 minutes at RT to block non-specific binding of immunoglobulin. Sections were incubated with iNOS primary antibody overnight at 4°C (Abcam; ab15323; 1:350 in blocking buffer) in a humidified chamber. Next day, slides were washed three times for 5 min in wash buffer (0.1% Tween20 in PBS). Sections were incubated with Alexa 568 secondary antibody (Invitrogen; A-11036) diluted 1:500 in blocking buffer for 30 minutes at RT in the dark and humidified chamber. Slides were rinsed in wash buffer three times for 5 minutes. Coverslips were mounted with Darko Fluorescence mounting medium (Darko, USA) onto slides. Slides were dried at least 1 day before imaging and kept at 4°C. Images were acquired using CLSM Leica SP5 microscope and LAS-AF 3.X software (Leica, Germany).

Isolation of the stromal vascular fraction from adipose tissue and flow cytometry

PVAT from thoracic aortae and epididymal adipose tissues (EFAT) were harvested, and digested enzymatically by incubation in a solution containing collagenase type D from clostridium histolyticum (0.5 mg/ml, Roche Diagnostics, Indianopolis, USA) dissolved in PBS supplemented with $CaCl_2$ 2.5 mmol/L for 1 hour at 37°C with constant agitation (900 rpm). After 30 minutes, tissues were passed 10 times through an 18g needle and, at the end of the incubation period, through a 30 µm sterile cell strainer (Miltenyi Biotec) to yield a single cell suspension corresponding to the vascular stromal fraction. Cells were washed and suspended in flow cytometry buffer (0.5% BSA, 1mM EDTA in PBS) containing of the following antibodies: fluorescein isothiocyanate anti-CD45.2 (1:200 Biolegend) and APC-AlexaFluor750 anti-F4/80 (1:100, Biosciences). After immunostaining (incubation with labeled antibodies for 40 minutes at 4°C in the dark), cells were washed 2 times in flow cytometry buffer and cell populations were analyzed by BD FACS Canto run with DIVA software (Becton Dickinson). Data were analyzed with FlowJo software 8.5.2, (Tree Star). Percentages of macrophages ($CD45^+$ $F4/80^+$) in the stromal vascular fraction from the different adipose tissues was determined.

Statistical Analysis

Data are expressed as means ± standard error of the mean (SEM). Vascular function experiments were analyzed with ANOVA for repeated measurements followed by a

Bonferroni post-hoc test. Contractions are given as a percentage of contraction to 100 mmol/L KCl, and dilations as a percentage of the maximal pre-contraction. pD2 (-log EC_{50}) values were calculated with non-linear regression analysis. Comparisons between groups for remaining experiments were analyzed by two-tailed Student's t-test. Differences were considered statistically significant at values of $P < 0.05$. All statistical analysis was performed using GraphPad Prism 5.04 program for Windows (GraphPad software, San Diego, CA, USA).

References

1. Cybulski N, Polak P, Auwerx J, Ruegg MA, Hall MN. Mtor complex 2 in adipose tissue negatively controls whole-body growth. *Proc Natl Acad Sci U S A*. 2009;106:9902-9907
2. Bhattacharya I, Ullrich A. Endothelin-1 inhibits adipogenesis: Role of phosphorylation of akt and erk1/2. *FEBS Lett*. 2006;580:5765-5771
3. Schmittgen TD, Livak KJ. Analyzing real-time pcr data by the comparative c(t) method. *Nat Protoc*. 2008;3:1101-1108
4. Bhattacharya I, Mundy AL, Widmer CC, Kretz M, Barton M. Regional heterogeneity of functional changes in conduit arteries after high-fat diet. *Obesity (Silver Spring)*. 2008;16:743-748
5. Mundy AL, Haas E, Bhattacharya I, Widmer CC, Kretz M, Baumann K, Barton M. Endothelin stimulates vascular hydroxyl radical formation: Effect of obesity. *Am J Physiol Regul Integr Comp Physiol*. 2007;293:R2218-2224
6. Garvey EP, Oplinger JA, Furfine ES, Kiff RJ, Laszlo F, Whittle BJ, Knowles RG. 1400w is a slow, tight binding, and highly selective inhibitor of inducible nitric-oxide synthase in vitro and in vivo. *J Biol Chem*. 1997;272:4959-4963

Supplementary Table 1

Primer list for quantitative real-time PCR

Gene	Forward primer (5'-3')	Reverse Primer (5'-3')
Arbp	AGCTGAAGCAAAGGAAGAGTCGGA	ACTTGGTTGCTTTGGCGGGATTAG
Rictor	TGCGATATTGGCCATAGTGA	ACCCGGCTGCTCTTACTTCT
Adipoq	GCACTGGCAAGTTCTACTGCA AACA	AGAGAACGGCCTTGTCCTTCTTGA
Retn	GCAAGGATAGACTGGACAGCA	AGACCGGAGGACATCAGACA
Inc2	CACCTCCATCCTGGTCAGGGA C	TCCGTGGTGGCCACTTGCAC
Nox2	AACTCCTTGGGTCAGCAGTG	GAGCAACACGCACTGGAAC
Nox4	GTGAAGATTTGCCTGGAAGAA C	TGATGACTGAGATGATGGTGAC
Il6	CCATCCAGTTGCCTTCTTG	AATTAAGCCTCCGACTTGTG
Mip1a	ACTGACCTGGAACTGAATGCCTGA	ATGTGGCTACTTGGCAGCAAACAG
Tnf	GCGGTGCCTATGTCTCAG	GCCATTTGGGAACTTCTCATC
Nos2	GCACCGAGATTGGAGTTC	AGCACAGCCACATTGATC
β-actin	CGTGCGTGACATCAAAGAGA	CCCAAGAAGGAAGGCTGGA

Insert missing primers

Supplemental Figures

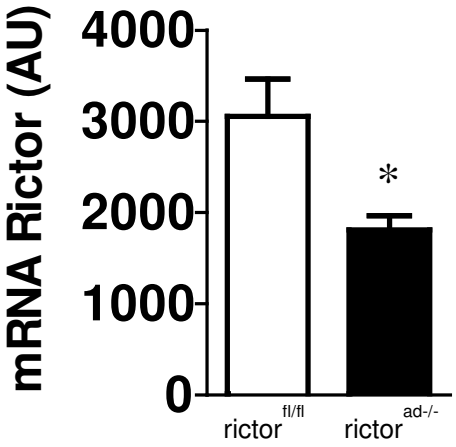

Supplemental Figure I: Steady state mRNA expression levels of rictor in epididymal fat were determined using quantitative real-time PCR in rictor $^{fl/fl}$ and rictor $^{ad-/-}$ mice. Data represent means ± SEM, n=5; *P<0.01.

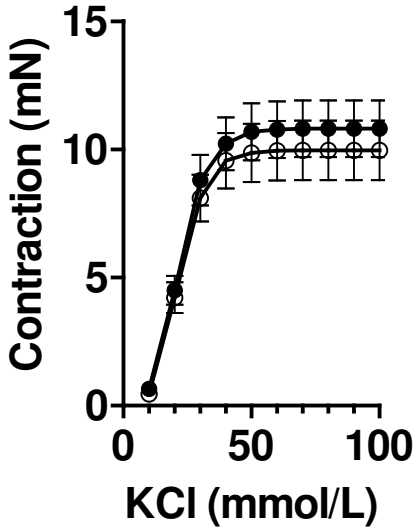

Supplemental Figure II: KCl-induced contractions. Aortic rings with PVAT from rictor$^{fl/fl}$ or rictor$^{ad-/-}$ mice were contracted with KCl in a concentration-dependent manner (10-100 mmol/L). Data represent means ± SEM, n=4-5.

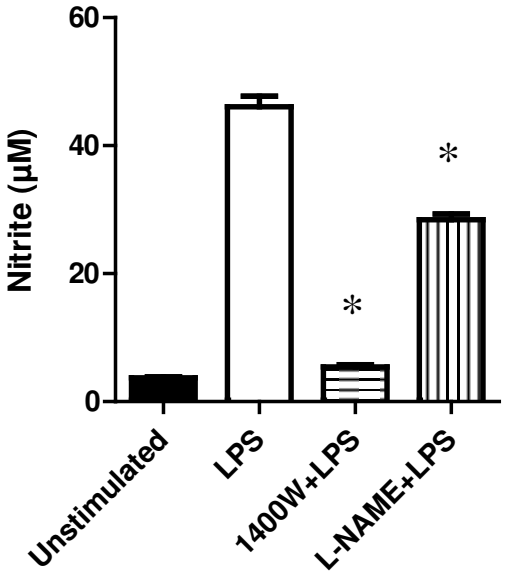

Supplemental Figure III: Inhibition of LPS-induced NO production by 1400W and L-NAME in macrophages. Murine macrophage RAW 264.7 cells were treated with 1400W (10^{-6} mol/L) or L-NAME ($300x10^{-6}$ mol/L). After 45 min, cells were stimulated with LPS (1 µg/ml) as indicated. Conditioned media was collected and nitrate levels were determined. Data represent means ± SEM, n=3; **P*<0.05 vs. LPS.

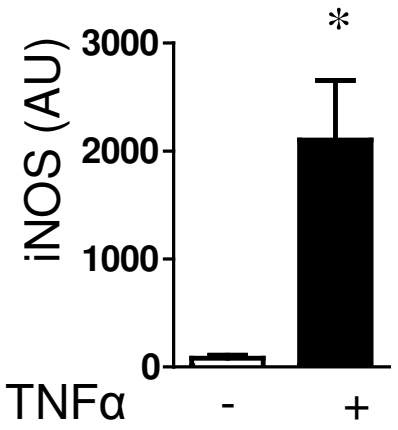

Supplemental Figure IV: TNFα stimulation increases gene expression of iNOS. Steady state mRNA expression levels of iNos were determined by quantitative real-time PCR in 3T3-L1 adipocytes stimulated with TNF (10 ng/ml). Values represent means ± SEM, n=5. *P<0.05

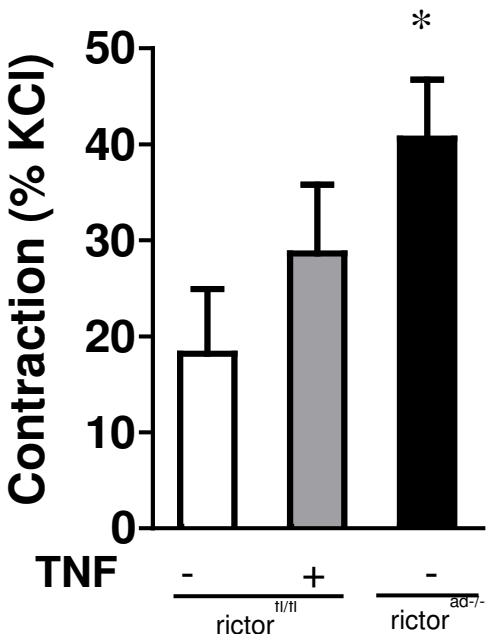

Supplemental Figure V: TNFα increases PE-mediated contration. Aortic rings with PVAT from rictor$^{fl/fl}$ mice were pre-treated with or without TNF (10 ng/ml) and then contracted with PE (10^{-6} mol/L). As reference, aortic rings with PVAT from rictor$^{ad-/-}$ mice were used Values are means±SEM, n=4; **P*<0.05 vs. rictor$^{fl/fl}$ without TNF.